A Continuously Updated Package-Degradation Model reflecting Thermomechanical Changes at Different Thermo-Oxidative Stages of Moulding Compound

Inamdar, A.S.; van Soestbergen, Michiel; Mavinkurve, Amar; van Driel, W.D.; Zhang, Kouchi

DOI
10.1109/EuroSimE56861.2023.10100833

Publication date
2023

Document Version
Final published version

Published in
2023 24th International Conference on Thermal, Mechanical and Multi-Physics Simulation and Experiments in Microelectronics and Microsystems, EuroSimE 2023

Citation (APA)
Inamdar, A. S., van Soestbergen, M., Mavinkurve, A., van Driel, W. D., & Zhang, K. (2023). A Continuously Updated Package-Degradation Model reflecting Thermomechanical Changes at Different Thermo-Oxidative Stages of Moulding Compound. In *2023 24th International Conference on Thermal, Mechanical and Multi-Physics Simulation and Experiments in Microelectronics and Microsystems, EuroSimE 2023* (2023 24th International Conference on Thermal, Mechanical and Multi-Physics Simulation and Experiments in Microelectronics and Microsystems, EuroSimE 2023). https://doi.org/10.1109/EuroSimE56861.2023.10100833

2023 24th International Conference on Thermal, Mechanical and Multi-Physics Simulation and Experiments in Microelectronics and Microsystems (EuroSimE) | 979-8-3503-4597-1/23/$31.00 ©2023 IEEE | DOI: 10.1109/EuroSimE56861.2023.10100833

A Continuously Updated Package-Degradation Model reflecting Thermomechanical Changes at Different Thermo-Oxidative Stages of Moulding Compound

Adwait Inamdar[1,*], Michiel van Soestbergen[2], Amar Mavinkurve[2], Willem van Driel[1,3], GuoQi Zhang[1]
[1] Delft University of Technology, Mekelweg 5, 2628 CD Delft, The Netherlands
[2] NXP Semiconductors, Gerstweg 2, 6534 AE Nijmegen, The Netherlands
[3] Signify, High Tech Campus 7, 5656 AE Eindhoven, The Netherlands
[*] a.s.inamdar-1@tudelft.nl ORCID: 0000-0002-9776-7499

Abstract

Moulding compounds used for encapsulating electronics typically occupy a large portion of package volume and are most exposed to the external environment. Under harsh conditions such as high temperature, humidity, and mechanical vibrations, constituent materials of electronic components degrade, resulting in a change in their thermal, mechanical, electrical, and chemical behaviour. High-temperature ageing of electronic packages causes the oxidation of epoxy moulding compounds (EMC), forming a layer exhibiting significantly different thermomechanical properties. This reflects in the modified mechanical behaviour of the entire package, which accelerates certain failure modes and affects component reliability. Thus, it is crucial to consider gradual degenerative changes in EMC for a more accurate estimation of the component lifetime.

This paper proposes a three-step modelling approach to replicate thermo-chemical changes in package encapsulation. A parametric geometry of a test package was incorporated with the ageing stage-dependent changes in thermomechanical properties of the oxidized layer. The mechanical behaviour of oxidized EMC at multiple stages of thermal ageing (at 150 °C for up to 3000 hours) was first experimentally characterized and then validated using warpage measurements on thermally aged test packages and Finite Element (FE) simulations. Lastly, a trend-based interpolation of material model parameters for intermediate stages of ageing was followed, and a continuously updated degradation model (physics-based Digital Twin) was achieved. The proposed model is capable of reproducing degraded stages of the test package under thermal ageing along with its modified thermomechanical behaviour. Its limitations and significance in the domain of health monitoring of microelectronics are also discussed.

1. Introduction

Epoxy-based thermosets, commonly known as moulding compounds, are widely used for packaging electronic circuits due to their desirable mechanical and chemical properties [1–3]. The encapsulating material is exposed to ambient conditions, which makes it most susceptible to degradation over time. Owing to its volume-share as high as 75% [4] within a typical electronic package, encapsulation tends to govern the overall mechanical behaviour of the package. Thus, degenerative changes in moulding compounds can significantly affect component lifetime.

Electronic components in certain applications need to withstand harsh environments. For example, the Automotive Electronic Council (AEC) standards define qualification tests involving temperature variation between −40 °C and 125 °C, mechanical vibrations with a peak acceleration of 50 g, and humid environments up to 85 % RH [5]. Among various environmental loads, exposure to high temperature is one of the biggest contributing factors to component degradation and eventual failures [6].

Thermal ageing is primarily reflected in the oxidation of epoxy moulding compound (EMC) through its contact with atmospheric oxygen, forming a layer of oxidized material up to a certain depth from the exposed surface. It has been established with Fourier Transform Infrared (FT-IR) spectroscopy measurements that the ageing process changes the material chemically [7, 8]. Moreover, the changes in thermomechanical properties of thermally aged EMC specimens have also been reported [9, 10].

Figure 1 shows the cross sections of thermally aged EMC specimens observed under a fluorescence microscope. Within a single specimen, the two different colours (refer to stage 3) indicate two distinct 'states' of EMC – pristine and oxidized; whereas the colour gradient (refer to stage 1) shows the gradual transformation from oxidized to pristine state. The difference in the colour composition

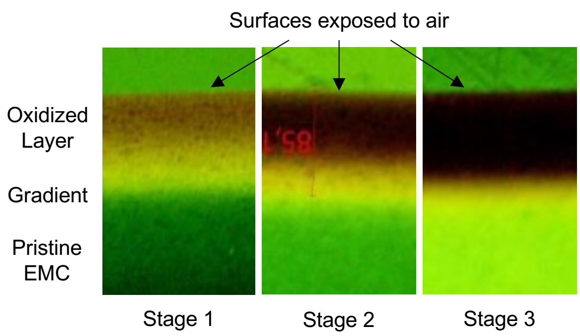

Figure 1. Cross sections of three different 'stages' of partially-oxidized EMC specimens observed under a fluorescence microscope.

of the oxidized layers across three different specimens highlights different 'stages' of EMC oxidation. As thermal ageing progresses, the oxidation layer grows in thickness, and the outer layer of EMC becomes more and more oxidized [11].

In general, the growth of oxidation thickness is time and temperature dependent [12]. At higher temperatures, the oxidation layer grows faster, resulting in a darker layer that is easier to distinguish. At lower temperatures, the oxidation layer grows slower, and a prominent gradient from pristine to oxidized state is observed. The temperature dependence of the ageing process is presented in references [10, 13, 14], where the cross sections of thermally aged EMC specimens indicate that the same storage time at different ageing temperatures results in different stages of EMC oxidation.

In the current work, we focus on the time dependence of the ageing process at 150 °C. Therefore, different ageing stages correlate to different storage times. Figure 2 illustrates different stages of EMC oxidation obtained by ageing bar-shaped specimens of EMC at a constant temperature. Note the gradual increase in thickness and the change in colour of the oxidized layer. The latter indicates changes in material properties.

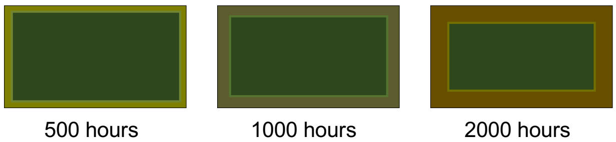

Figure 2. Schematic representation of the oxidized EMC layer at the cross sections of isothermally aged bar-shaped EMC specimens.

In the case of a thermally aged electronic package, the outer layer of EMC is oxidized. This outer shell exhibits modified thermomechanical properties and changes the mechanical behaviour of the entire package. This can accelerate certain failure modes, such as delamination along the EMC-die interface, cracks in the bulk of EMC [7], and fatigue failure of solder joints [15]. Thus, quantifying gradual degenerative changes within EMC (here, determining the current stage of EMC oxidation) becomes crucial. This can be addressed by two aspects of a thermally aged stage – the thickness of the oxidized layer and its thermomechanical properties at the current stage.

This paper presents a methodology to prepare an experimentally validated model for predicting the progress of EMC oxidation in an electronic package due to High-Temperature Storage (HTS). It consists of three steps – (1) modelling the degradation mechanism, (2) modelling a parametric geometry of the Device Under Test (DUT), and (3) modelling the ageing-stage-dependent material behaviour. Finally, an approach for trend-based interpolation of thermomechanical properties for the intermediate stages of oxidized EMC is proposed to obtain a continuously updated package-degradation model.

2. Modelling Degradation Mechanism

EMC oxidation is a combination of two processes – the diffusion of oxygen into the free volume of the polymer network and the chemical reaction of oxygen with the resin. In the case of thermal ageing at a constant temperature, the thickness of the resulting oxidation layer defines a particular ageing stage. Thus, the Thickness of the Oxidation Layer (TOL) was experimentally measured as a function of storage time (t). Bar-shaped EMC specimens (80 mm × 10 mm × 4 mm) were thermally aged for up to 3000 hours at 150 °C, which is above the glass transition temperature (T_g) of the selected EMC. The aged (partially-oxidized) specimens were cross-sectioned and observed under a fluorescence microscope with UV illumination. TOL was measured at multiple locations within each specimen, and the mean value was recorded. Figure 3 shows the measured data in red.

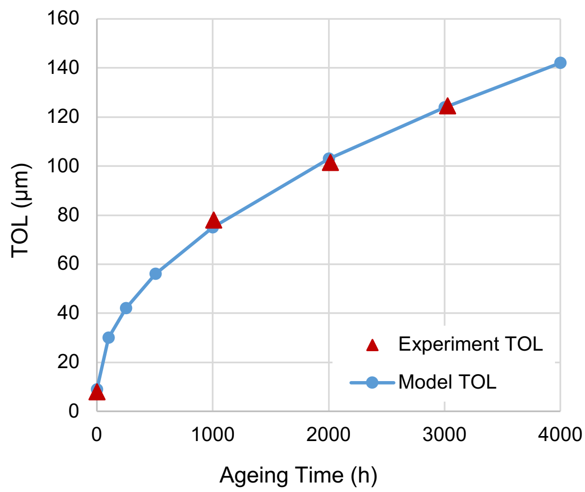

Figure 3. Experimentally measured TOL data fitted to the oxidation layer growth model $d = d_0 + d_1 t^n$, where $n = 0.5$, $d_0 = 8.7132\,\mu m$, and $d_1 = 2.1053\,\mu m$.

The oxidation process is also referred to as Diffusion Limited Oxidation (DLO) because the oxidized layer acts as a barrier for further diffusion of the atmospheric oxygen. Thus, EMC oxidation is often modelled as a diffusion-dominant process with a direct proportionality to the square root of time [11], i.e. $d \propto \sqrt{t}$, where d is the TOL. The above relation was considered the basis for the oxidation growth model.

The proposed degradation model takes the form of the equation (1), where d_0, d_1, and n are fitting parameters.

$$d = d_0 + d_1 t^n \tag{1}$$

Instead of directly using the square root of time, a slightly more flexible version with $n \in (0, 1)$ was used as a starting point. A non-zero value of the parameter d_0 reflects the oxidation thickness ($\approx$ 9 µm) at $t = 0$ due to the processes like Post Mould Cure (PMC) prior to the ageing experiment.

A standard curve fitting procedure was followed to determine the parameter values ($d_0 = 8.7132\,\mu m$, $d_1 = 2.1053\,\mu m$, and $n = 0.5$). Interestingly, the value deduced for the parameter n is exactly equal to 0.5. The oxidation growth model fitted to the experimental data is indicated in Figure 3, along with some additional TOL values (marked blue) calculated using the finalized model.

3. Modelling Parametric Geometry

The second step is to prepare a geometric model of the Device Under Test (DUT) such that it can be updated to reflect the current degradation state. A Quad-Flat No-leads (QFN) package with a flip-chip construction (i.e., die-substrate interconnects using copper pillars with solder caps) was chosen as the DUT. Initially, the geometry of a non-aged package was constructed with some select simplifications.

The package substrate has a total of five layers (three metallization layers and two intermediate layers for copper vias), each of which was modelled as individual homogeneous layers. Layer-wise equivalent material properties were calculated using the volume-based weighted average of the (linear elastic temperature dependent) mechanical properties of the copper and utilized polymer. Moreover, the copper pillars and solder caps in the flip-chip construction were modelled in detail as cylindrical structures. The EMC encapsulates only the die and die-substrate interconnects (including underfill) and rests on the substrate (does not encapsulate the substrate).

To reflect the growth of the oxidation layer within EMC, a single parameter was defined to represent the current value of TOL. It was assumed that the oxidation layer grows uniformly in directions perpendicular to all exposed surfaces of EMC, which is a good representation of reality. The required computational effort was reduced by using a quarter geometry. Figure 4 indicates the core-shell style geometry of a thermally aged package.

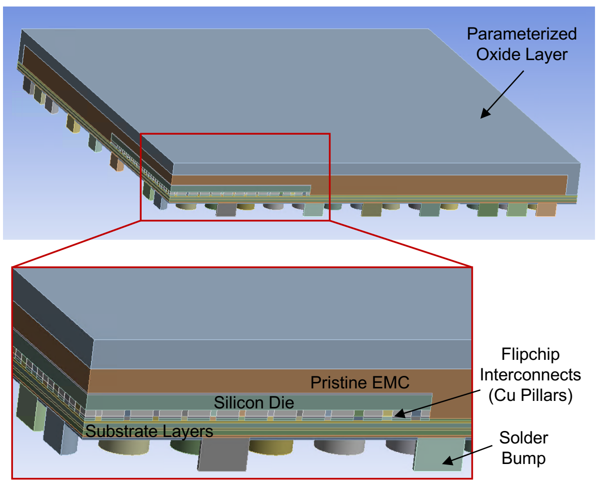

Figure 4. Quarter geometry of a thermally aged DUT indicating its sub-layers including a parameterized layer for oxidized EMC.

A parametric setting was utilized along with an automation routine to update the geometric model with the TOL for different stages of EMC oxidation. Appropriate settings were applied to maintain the mesh quality for all stages of ageing at 150 °C for up to 3 years. At any given ageing stage, corresponding material properties of the oxidized EMC (discussed in the following section) were assigned to the oxidized layer.

4. Modelling Thermomechanical Properties of EMC at Several Oxidation Stages

To determine the change in thermomechanical properties of the oxidized EMC due to ageing, an approach of using partially-oxidized EMC specimens for experimental characterization followed by an analytical solution to calculate the effective properties of the oxidized layer was pursued.

Two sets of bar-shaped EMC specimens were thermally aged at 150 °C for 0 h, 500 h, 1000 h, 1500 h, 2000 h, 2500 h, and 3000 h. For each ageing stage, the modulus of elasticity (E) was characterized using a single-frequency Dynamic Mechanical Analysis (DMA) at 1 Hz on the first set of aged specimens (80 mm × 10 mm × 4 mm); whereas the Coefficient of Thermal Expansion (CTE) and the shift in the glass transition temperature were characterized using Thermal-Mechanical Analysis (TMA) on the second set of thermally aged specimens (15 mm × 4 mm × 3 mm). In this way, the experimental data of linear elastic temperature-dependent material properties for the pristine (0 h aged specimens) and different partially-oxidized EMC specimens were gathered.

Elastic Modulus of Oxidized EMC

The elastic properties of the oxidized layer at each ageing configuration were derived from the experimental data using the flexural equation extended for multi-material composite beams [7]. In this case, the cross-section of a partially-oxidized beam specimen consists of a 'core' pristine layer (thickness h_{pr}) sandwiched between two 'shell' oxidized layers (thickness h_{ox} each). The analytical calculation considers the oxidation layer only on the top and bottom of the pristine layer. Thus, the total beam thickness is $h = h_{pr} + 2\,h_{ox}$.

Equating the bending moment at a cross-section of an equivalent homogeneous beam with that of a composite beam and applying strain-continuity (and discontinuous stress) across different layers within the cross-section, the relation between effective elastic properties and that of individual layers boils down to the equation (2), where E_{eff}, E_{pr}, E_{ox} are moduli of elasticity, and I_{eff}, I_{pr}, I_{ox} are the corresponding area moment of inertia, for the effective beam (partially-oxidized specimen), 'core' of the composite beam (pristine EMC), and 'shell' of the composite beam (oxidized EMC), respectively.

$$E_{eff}\,I_{eff} = E_{pr}\,I_{pr} + E_{ox}\,I_{ox} \quad (2)$$

$$\implies \quad E_{eff}\,h^3 = E_{pr}\,h_{pr}{}^3 + E_{ox}\,(h^3 - h_{pr}{}^3) \quad (3)$$

Due to the common width, the equation (2) gets further simplified to the equation (3), based on which the values for E_{ox} at different ageing stages were evaluated using the linear elasticity data of E_{pr} and E_{eff}.

A mathematical model of the form given in the equation (4) was fitted to the elasticity curves to model the dependency on temperature (T); where $f \in (0,1)$, r, and s are fitting parameters; T_g^{ox} is glass transition temperature; E_g^{ox} is glassy modulus; E_r^{ox} is the rubbery modulus of the oxidized EMC at a particular ageing-stage.

$$E_{ox}(T) = E_r^{ox} + E_g^{ox}\, f\, \exp\left[-10^{-\left(\frac{T_g^{ox} - T + s}{r}\right)}\right] \quad (4)$$

Standard curve fitting techniques were utilized to obtain the values of the fitting parameters f, r, and s at different ageing stages. For the pristine EMC, their values are $f = 0.938$, $r = 41.847$, and $s = 16.044$; whereas for all oxidized stages, they are $f = 0.725$, $r = 63.354$, and $s = 11.803$. Figure 5 shows the fit of the finalized material model to the experimentally evaluated E_{ox} data.

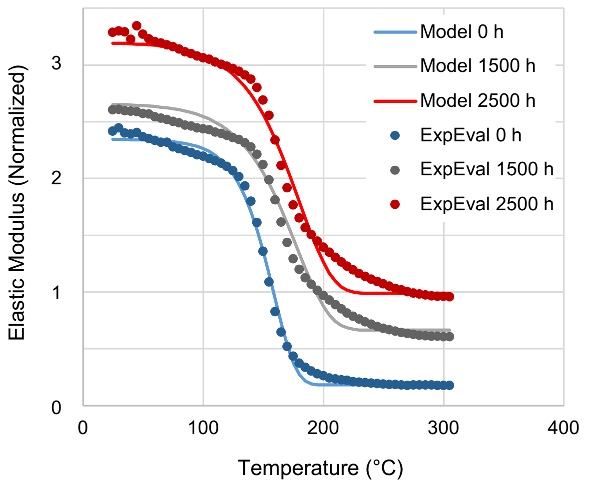

Figure 5. Linear elastic temperature-dependent material model fitted to the experimentally evaluated elasticity data of the oxidized EMC layer at three stages of thermal ageing at 150 °C.

The elasticity curves for the oxidized EMC at any oxidation stage can now be obtained by determining the values of material-model parameters T_g^{ox}, E_g^{ox}, and E_r^{ox}. Thus, the parameterization of the material model is an important step in introducing continuity in different oxidation stages, more of which is described later in Section 6.

CTE and T_g of Oxidized EMC

Evaluating the CTE (α) of the oxidized EMC from partially-oxidized EMC specimens is not straightforward. The TMA test generally focuses on measuring only the change in the (dimension along the) length, while a bonded bi-material strip also shows a bending deformation due to a CTE mismatch between layers. Thus, the CTE calculation for a multi-material system requires more complex equations, including the moduli of elasticity of the involved layers. The relation between the thermal expansion-induced curvature of a bi-material strip and the properties (E and α) of its constituting materials is derived in the reference [16].

However, the partially-oxidized EMC specimens used here are symmetrically oxidized (from both the upper and lower surfaces of the beam). They, therefore, are not expected to show bending due to the CTE mismatch. Thus, available values of α_{pr} and α_{eff} from the TMA test results were utilized to calculate α_{ox} at different ageing stages using a volume-based weighted average as indicated in the equation (5), which has also been used in the previous publication [7].

$$h\,\alpha_{eff} = h_{pr}\,\alpha_{pr} + (h - h_{pr})\,\alpha_{ox} \quad (5)$$

The T_g is typically determined from the thermal strain vs temperature curves obtained from a TMA test. But in this case, the T_g obtained from the TMA test would correspond to the whole partially-oxidized EMC specimen (T_g^{eff}) and not to the oxidized layer. Thus, the T_g^{ox} of each oxidized stage was derived from the evaluated elastic modulus values (E_{ox} vs T) based on the DMA results.

In this way, the linear elastic thermomechanical behaviour model was obtained for the oxidized EMC at different stages of thermal ageing. Note that the above procedure provides initial estimates of the α_{ox} and T_g^{ox} values, which need to be updated with an experimental validation using the DUT.

5. Experimental Validation of Behavioural Model

Experiments were designed around thermally aged DUT specimens to validate the behavioural model. The packages were stored at 150 °C for several ageing intervals up to 3000 h. Then, the warpage of aged DUTs was measured at various temperatures between 25 °C (room temperature) and 260 °C at a heating rate of 60 K/min. In this context, the warpage indicates the out-of-plane deformation (along the Z-direction) measured on the top surface (XY plane) of the package.

A finite element simulation was set up on the parametric geometry of the DUT to reflect the experimental load conditions. A diagonal path was defined along the top surface of the package, and the warpage along that path was extracted from the FE results. Figure 6 shows the warpage evaluation path in the simulation and the experimental setting. The largest (in magnitude) out-of-plane deformation value along the diagonal path was recorded as the maximum warpage (Deformation Z) at several temperature values.

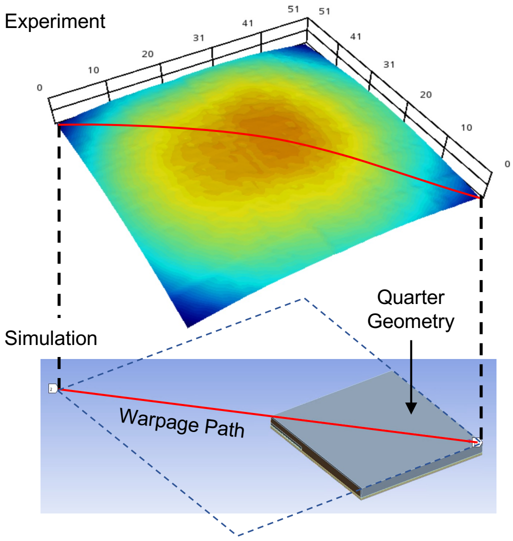

Figure 6. Experimental validation of the material model using warpage measurements along a diagonal path on the top surface of a thermally aged package. [Note: the spatial plot corresponds to the out-of-plane deformation at 100 °C of a package at the ageing stage of 1000 h.]

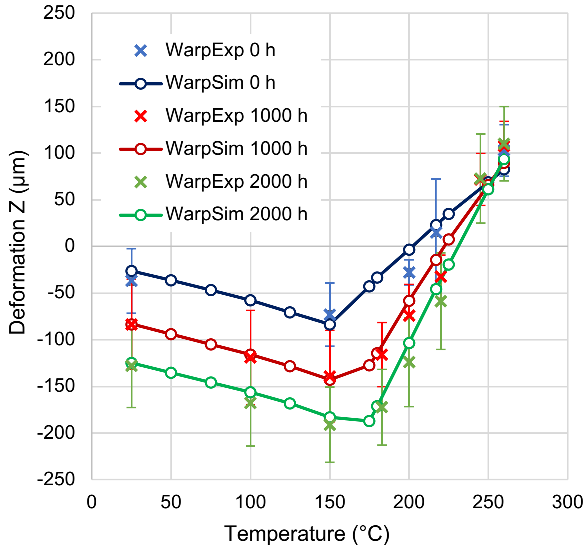

Figure 7. Maximum warpage data obtained from experimental measurements and corresponding FE simulations using the validated material models at three stages of thermal ageing – 0 h, 1000 h, and 2000 h.

The warpage during a temperature variation primarily originates from the CTE-mismatch (α) among different layers of the package, which is also linked with the glass transition of EMC. Since the utilized values of α_{ox} and T_g^{ox} were estimated based on the analytical approach described in Section 4, the initial simulation-based results showed a noticeable mismatch with the experimental trends. Thus, the two parameters α_{ox} and T_g^{ox} should be revised within an acceptable range.

Another reason for this mismatch is the curing shrinkage of EMC after the moulding process (and during PMC), which contributes to some additional warpage of the package. To reflect the shrinkage into the FE simulation, the stress-free reference temperature of just the EMC material (T_e) can be assigned a value higher than the rest of the package. As a starting point, the stress-free reference temperature (T_{ref}) of 180 °C was assigned to all components of the geometry, including the EMC. This was then rectified by setting the T_e for pristine EMC to 190 °C.

Moreover, it has been reported that during thermo-oxidative changes, EMC undergoes additional shrinkage [17]. This was taken into account by setting the T_e of the oxidized EMC layer to an even higher value (> 190°C) than that of the pristine EMC. This was independently done for each oxidized stage of EMC.

In this way, the material model parameters T_e^{ox}, T_g^{ox}, and α_2^{ox} (CTE after the glass transition) were updated over multiple iterations of FE simulations until a good match was found with experimental results. Figure 7 shows the experimentally measured maximum warpage against the simulation-based results based on the final validated model at three different ageing stages.

6. A Continuously Updated Model (Digital Twin)

Validated material models can simulate the package behaviour at only a select number of ageing stages. There are practical limitations to the number of such ageing stages for which the entire cycle of experimental and simulation-based study can be carried out. Therefore, it makes sense to interpolate the material behaviour for the intermediate 'unknown' stages based on the (validated material models at the) 'known' stages of ageing. This would essentially formulate a continuous material model for all stages of the oxidized EMC.

For this study, the continuity within EMC-oxidation stages was achieved by defining values for the material model parameters (such as α_{ox}, T_g^{ox}, T_e^{ox}, E_g^{ox}, E_r^{ox}) at intermediate ageing stages (here, the ageing time t). However, they cannot simply be linearly interpolated between two known stages. Each parameter shows a unique trend, especially in the early stages of ageing (from 0 h to 1000 h). This needs to be carefully considered for every material model parameter.

Overall, thermomechanical changes in the oxidized EMC tend to saturate beyond 2500–3000 h of ageing. Most material model parameters show a trend of rapid initial growth, slow increase, and saturation. But these three phases don't necessarily appear at the same ageing time for every parameter. Thus, additional information was sourced from the literature regarding the glass transition, shrinkage, and other parameters, and accordingly, their intermediate values were defined.

For example, experimental trends of EMC shrinkage during oxidation in references [14, 18] indicate a very sharp initial growth within about 100 h of ageing followed by a near-constant saturation value. To reflect this shrinkage trend, additional data points for T_e^{ox} were created. Figure 8 shows the development of T_e^{ox} as a function of ageing time. Red markers indicate values from the validated material models; the trend-based intermediate values are marked in blue.

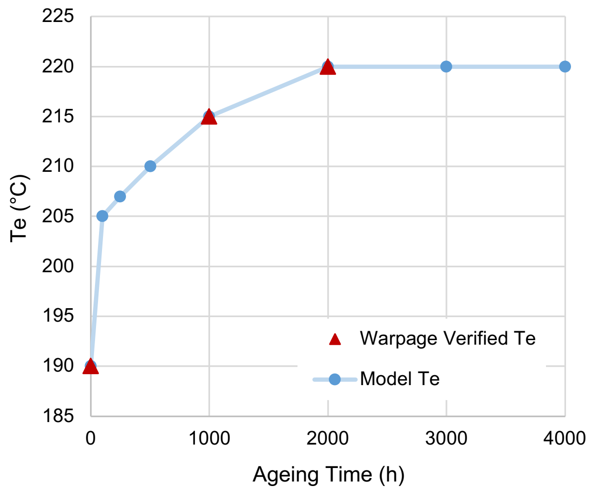

Figure 8. Values of the parameter T_e^{ox} at different ageing stages (trend line is only indicative of continuity). T_e^{ox} is the reference temperature of the oxidized EMC to account for the oxidation-induced shrinkage.

Elasticity-related material parameters (E_g^{ox} and E_r^{ox}) showed different trends. The glassy modulus stays nearly the same up to 1000 h of ageing but later shows a linear growth up to 3000 h. On the other hand, the rubbery modulus shows a more or less linear trend until 3000 h. Figure 9 shows E_r^{ox} as a function of ageing time, including the results evaluated from experimental characterization at different ageing stages.

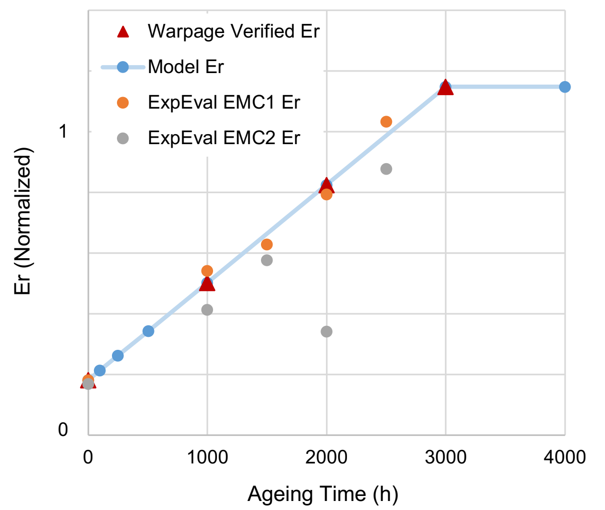

Figure 9. Rubbery modulus of the oxidized EMC as a function of ageing time for different stages of ageing, including experimental results.

The shift in the elasticity curves for partially-oxidized EMC specimens tends to slow down and eventually saturate after a particular ageing time. Since this change is essentially due to the changes in the oxidized layer, elasticity curves of the oxidized EMC were assumed to be constant after the 3000 h ageing stage. Figure 10 shows the linear elastic temperature-dependent elasticity model

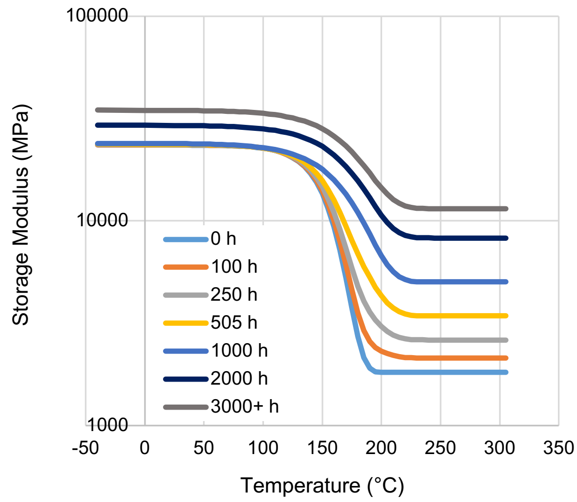

Figure 10. Temperature-dependent elastic modulus of the oxidized EMC at several stages of ageing.

(storage modulus) for the oxidized EMC, including several intermediate stages between 0 h and 1000 h.

In this way, a continuous material model was developed, which reflects gradual changes in the thermomechanical behaviour of the oxidized EMC. Combining this with the degradation model (Section 2) and package geometry (Section 3), a continuously updated package-degradation model (i.e., a physics-based Digital Twin) is achieved.

7. Summary and Conclusion

This study presents a three-step procedure for modelling thermal ageing-induced EMC oxidation in a flip-chip QFN package and the corresponding changes in the thermo-mechanical behaviour. First, the growth of the oxidation layer was measured using thermally aged (150 °C) EMC specimens and a diffusion-dominant mathematical model was fitted to the data. Second, a parametric geometry of the DUT was prepared to reflect the oxidation layer growth at ageing stages up to 3 years. Finally, a systematic procedure was followed to characterize the thermomechanical properties of partially-oxidized EMC specimens experimentally and then to analytically deduce the equivalent properties of only the oxidized layer at multiple stages of ageing. Obtained behavioural models were validated and updated by comparing FE simulation results with warpage experiments. The continuity in the behavioural model was achieved by defining material model parameters (α, T_g, T_e, E_g, E_r) as functions of ageing-time (t), considering their individual trends.

A continuously updated package-degradation model (in other words, a physics-based Digital Twin) consists of an oxidation growth model, a parametric DUT geometry, and a continuous behavioural model. Knowing the duration of exposure to high-temperature (150 °C), the Digital Twin can be updated to represent the current condition of a thermally aged DUT package more accurately. The updated model can then be utilized for a Finite Element Analysis (FEA) to predict the likeliness of failure modes associated with the changed mechanical behaviour of the package in the current state of degradation. Digital Twin-based lifetime prediction is a key component of the modern implementation of the Prognostics and Health Management (PHM) framework, especially for mission-critical electronics.

The current model has its own set of limitations and can be significantly improved by including a few more validated ageing stages between 0 h and 1000 h. The presented methodology can be extended to include a viscoelastic behavioural model instead of a linear elastic one for the (oxidized) EMC. Future work is planned to carry out a simulation-based study to investigate the effect of oxidation growth on the room-temperature warpage and EMC-die interface stresses in the context of delamination.

Acknowledgement

This work has been carried out within the project ArchitectECA2030 under the grant agreement №877539. The project is co-funded by grants from Germany, Netherlands, Czech Republic, Austria, Norway and Electronic Component Systems for European Leadership Joint Undertaking (ECSEL JU).

The authors would also like to thank Sumitomo Bakelite for performing the thermal ageing, conducting thermomechanical analysis, and supplying the samples for further characterization. Furthermore, we are grateful to Leon Goumans (NXP, Nijmegen) for performing the oxidation thickness measurements with fluorescence microscopy. Finally, C.S. Foong (NXP, Austin) is also gratefully acknowledged for providing the package warpage data.

References

[1] M. J. Mullins, D. Liu, and H. J. Sue. Mechanical Properties of Thermosets. In Qipeng Guo, editor, *Thermosets: Structure, Properties and Applications*, chapter 2, pages 28–61. Woodhead Publishing, 2012.

[2] D. Carolan, A. Ivankovic, A. J. Kinloch, S. Sprenger, and A. C. Taylor. Toughening of epoxy-based hybrid nanocomposites. *Polymer*, 97:179–190, 8 2016.

[3] Haleh Ardebili, Jiawei Zhang, and Michael G. Pecht. *Encapsulation Technologies for Electronic Applications*. Elsevier, second edition, 2018.

[4] Yong Liu. *Power Electronic Packaging*. Springer New York, 2012.

[5] AEC-Q100-Rev-H FAILURE MECHANISM BASED STRESS TEST QUALIFICATION FOR INTEGRATED CIRCUITS Component Technical Committee Automotive Electronics Council, 2014.

[6] Richard C. Chu, Robert E. Simons, Madhusudan Iyengar, and Lian-Tuu Yeh. Thermal Management of Flip Chip Packages. In Tong Ho-Ming, Lai Yi-Shao, and Wong C.P., editors, *Advanced Flip Chip Packaging*, volume 9781441957, chapter 9, pages 413–469. Springer, Boston, MA, 8 2013.

[7] A Mavinkurve, L Goumans, and J Martens. Epoxy molding compounds for high temperature applications. In *2013 Eurpoean Microelectronics Packaging Conference (EMPC)*, pages 1–7, 2013.

[8] Pradeep Lall, Shantanu Deshpande, Yihua Luo, Mike Bozack, Luu Nguyen, and Masood Murtuza. Degradation mechanisms in electronic mold compounds subjected to high temperature in neighborhood of 200°C. In *Proceedings - Electronic Components and Technology Conference*, pages 242–254. Institute of Electrical and Electronics Engineers Inc., 9 2014.

[9] J. De Vreugd. *The effect of aging on molding compound properties*. PhD thesis, Delft University of Technology, 6 2011.

[10] Bingbing Zhang. *Material Characterization, Modelling and Simulation of Epoxy Moulding Compounds under High Temperature Storage and Temperature Cycling Thermal Ageing*. PhD thesis, Universität der Bundeswehr München, 11 2020.

[11] Eric Nguegang. *Experimental and Simulation-based Investigations on the Influence of Thermal Aging and Humidity on the Warpage of Molded Plastic Packages*. PhD thesis, University of Stuttgart, 4 2013.

[12] Adam Quintana and Mathew C. Celina. Overview of DLO modeling and approaches to predict heterogeneous oxidative polymer degradation, 3 2018.

[13] A. Inamdar, Y.-H. Yang, A. Prisacaru, P. Gromala, and B. Han. High temperature aging of epoxy-based molding compound and its effect on mechanical behavior of molded electronic package. *Polymer Degradation and Stability*, 188, 2021.

[14] Luca Grandi and Marco Rovitto. Thermal Aging on Molding Compounds: Material Characterization and Modeling. In *2022 23rd International Conference on Thermal, Mechanical and Multi-Physics Simulation and Experiments in Microelectronics and Microsystems, EuroSimE 2022*. Institute of Electrical and Electronics Engineers Inc., 2022.

[15] A. Inamdar, P. Gromala, A. Prisacaru, A. Kabakchiev, Y. Yang, and B. Han. EMC Oxidation Under High-Temperature Aging. In W.D. van Driel and M.Y. Mehr, editors, *Reliability of Organic Compounds in Microelectronics and Optoelectronics*, pages 53–80. Springer, Cham, 2022.

[16] T. W. Clyne. Residual Stresses in Surface Coatings and Their Effects on Interfacial Debonding. *Key Engineering Materials*, 116-117:307–330, 12 1995.

[17] L. Olivier, C. Baudet, D. Bertheau, J. C. Grandidier, and M. C. Lafarie-Frenot. Development of experimental, theoretical and numerical tools for studying thermo-oxidation of CFRP composites. *Composites Part A: Applied Science and Manufacturing*, 40(8):1008–1016, 8 2009.

[18] Leo Ernst. Refreshing Fracture Mechanics and High Temperature Aging of EMC, 2016.